

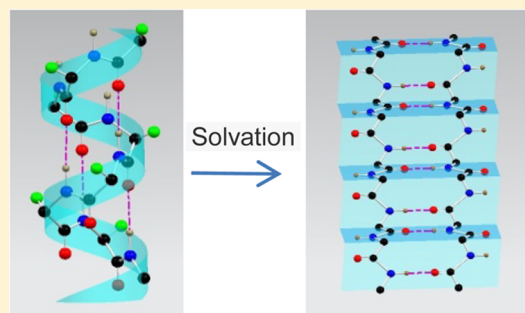
# Conformational Change of Bovine Serum Albumin Molecules at Neutral pH in Ultra-Diluted Aqueous Solutions

Shulian He, Mei Huang, Wei Ye, Dechao Chen, Shuai He, Liping Ding, Yunjin Yao, Lei Wan, Jinzhang Xu, and Shiding Miao\*

Anhui Key Lab of Controllable Chemical Reaction & Material Chemical Engineering, School of Chemical Engineering, Hefei University of Technology, Tunxi Road 193, 230009, Hefei, Anhui, China

## S Supporting Information

**ABSTRACT:** Surface chemical and electrochemical techniques were applied to reveal the unfolding of bovine serum albumin (BSA) molecules induced by concentrations in aqueous solution. Real-time surface pressures vs time ( $\pi$ - $t$ ) kinetic curves were recorded over an aqueous subphase (190 mL) by spreading BSA solutions of different concentrations but of the same amount ( $8.0 \times 10^{-4}$  mg) at the air/water (A/W) interface. A critical concentration ( $\sim 1.0$  ppm) was discovered below which the surface pressure declines with time and the BSA is totally solubilized in the water subphase. Above this critical concentration (e.g., 8.0 ppm), the surface pressure goes up and the protein molecules assemble into a Langmuir monolayer at the A/W interface. These findings demonstrate that the BSA molecules have different conformations in the spreading protein solutions. The conformational transition in BSA molecules induced by concentrations was also confirmed by spectroscopy means and the catalytic hydrogen evolution reaction on a silver amalgam electrode by using constant current chronopotentiometric stripping. This discovery fills in gaps of Foster's N (normal)  $\rightarrow$  F (fast) model, in which the unfolding of BSA molecules occurs at neutral pH values (8.0–4.3).



## INTRODUCTION

Understanding the structural conformations or protein unfolding will aid the development of immune technology for the exploitation of their use in biocatalysis.<sup>1</sup> However, protein folding always involves subtle changes in energy (usually  $<15$  kcal·mol<sup>-1</sup>), whereby some intermediate states are unstable in most cases.<sup>2</sup> It is a real challenge to characterize these intermediate states, as their instantaneous appearance depends on the conformation transformations. An example is bovine serum albumin (BSA) which is one of the most widely used proteins, and has been studied intensively in the past decades.<sup>3</sup> A famous model proposed by Foster is the N (normal)  $\rightarrow$  F (fast)  $\rightarrow$  E (expanded) transitions induced by pH values, in which BSA molecules are dissolved in aqueous solutions.<sup>4–6</sup> The BSA molecules undergo isomer transitions of N  $\rightarrow$  F  $\rightarrow$  E with decreasing pH (8.0  $\rightarrow$  4.3  $\rightarrow$  2.7). More conformational isomers (B (basic) form, pH 8.0–10; A (aged) form, pH  $> 10$ ) of BSA were found in alkaline solutions.<sup>7,8</sup> A great number of protocols including streaming birefringence,<sup>4</sup> viscometry,<sup>9</sup> small-angle scattering,<sup>10</sup> circular dichroism (CD),<sup>11</sup> electron microscopy,<sup>12</sup> fluorescence spectroscopy,<sup>13</sup> constant current chronopotentiometric stripping (CPS),<sup>14</sup> etc., have been applied to reveal these conformational/configurational transitions of BSA molecules. Despite this large number of investigations that have been performed on transitions of BSA structures induced by pH values, ionic strength, presence of surfactants or lipids, and references therein,<sup>7,8,15,16</sup> factors of

hydrated water shells are still major subjects of many experimental and theoretical investigations.<sup>17–19</sup> Conformational changes on the protein secondary and tertiary structures induced by the effect of water, which is the most common medium for the protein to be dissolved, have been less studied. Up to now, only a few studies have been conducted in which the conformation changes of interfacial protein molecules have been mentioned; however, not much detailed information about these molecular level changes that are dependent on concentrations has been provided,<sup>20,21</sup> and, sometimes, the conclusions are even controversial.<sup>22–24</sup>

Proteins can be considered as a special group of amphiphilic molecules, and they tend to form Langmuir monolayers at the air/water (A/W) interface even without the assistance of surfactants.<sup>24–26</sup> In our previous study, films of water-soluble proteins (lysozyme and BSA) have been prepared by spreading aqueous solutions of proteins over water in a Langmuir–Blodgett (LB) trough.<sup>25,27–29</sup> From these preliminary studies, we know that BSA molecules segregate at the A/W interface immediately at a concentration higher than 8.0 ppm (mg·mL<sup>-1</sup>), and the surface coverage increases with the concentration of the spreading solution.<sup>22,25</sup> In this study, the conformation of BSA molecules at a lower concentration was

Received: August 11, 2014

Revised: September 23, 2014

Published: September 29, 2014

investigated. We found that the unfolding of BSA molecules can be induced by another important factor, the concentration, which was omitted by the previous reports. Factors such as pH values, ionic strength, surfactants, and lipids have been well reported in the literature;<sup>7,8,15,16</sup> however, to the best of our knowledge, the finding on concentration-induced protein conformational change is for the first time reported by us in this report. The unfolding effect of BSA molecules is observable especially in ultra-diluted aqueous solutions. A critical concentration of  $\sim 1.0$  ppm was discovered across which the protein goes from a folded native structure to an unfolded isomer when the solution of BSA was diluted from 8.0 to 0.8 ppm. An expansion of the BSA molecule was confirmed by the surface chemical technique. We have revealed that extra-molecular hydrogen bonds formed between proteins and water molecules actually loosen the structure of the protein molecules, and this accounts for a solubility enhancement of BSA in aqueous solutions. The unfolding of BSA molecules was also confirmed by the CD, the attenuated total reflectance FTIR spectroscopy (ATR-FTIR), the atomic force microscopy (AFM), and electrochemical means.

## ■ EXPERIMENTAL SECTION

**Materials and Chemicals.** Bovine serum albumin (BSA) (99%) was purchased from Sigma-Aldrich. The lyophilized powders with an average molar molecular weight of  $\sim 67$  kDa were used as received. The isoelectric point of the protein was approximately 4.7. Disodium hydrogen phosphate ( $\text{Na}_2\text{HPO}_4$ ), sodium dihydrogen phosphate ( $\text{NaH}_2\text{PO}_4$ ), and other chemicals of analytical purity were provided by Sinopharm Chemical Reagent Co. China. The stock solution of BSA was prepared by dispersing 10.0 mg of BSA in 100.0 mL of Millipore (MQ) water (18.2 M $\Omega$ , surface tension of 72.6 mN $\cdot$ m $^{-1}$  at  $25.0 \pm 0.5$  °C, pH 6.8–7.2) and stored in the refrigerator at a temperature of +4 °C. Before each experiment, a known volume of the stock BSA solution was diluted to a determined concentration with MQ water. Phosphate-buffered saline (PBS) with a total ionic strength of 0.02 M was utilized to control the pH of buffer solutions. An internal reflection element (ZnSe crystal) served as the substrate for sample deposition in the FTIR spectroscopy measurement, and it was cleaned ultrasonically in acetone. Quartz cells or slides were used for protein solutions and LB films in the CD measurement, and were cleaned in the piranha solution (mixture of  $\text{H}_2\text{SO}_4$  (98%) and  $\text{H}_2\text{O}_2$  (35%) with a ratio of 7:3, v/v) for 30 min at 90 °C. Glass slides (10  $\times$  10 mm $^2$ ) were used for AFM characterization, and were cleaned via the same method as quartz slides.

**$\pi$ -t Curves,  $\pi$ -A Isotherms, and LB Film Deposition.** A LB trough (volume 190 mL, ZhongChen Co.) made of Teflon was used in this research. The apparatus has a pair of mobile poly(tetrafluoroethylene) barriers for compressing the monolayer at the A/W interface and a Wilhelmy balance employed for measuring the surface pressure ( $\pi$ ). Langmuir films of proteins were prepared over the MQ water or a buffer solution. A volume of BSA solution with a specific concentration was spread at the A/W interface by a syringe. After spreading, a period of time was allowed to achieve a stable surface pressure. During the period, the kinetics in the formation of the Langmuir monolayer was recorded by monitoring the surface pressure vs time ( $\pi$ -t). After equilibrium, the Langmuir film was compressed and the  $\pi$  vs monolayer area isotherm ( $\pi$ -A) was recorded to evaluate the area of the proteins at the A/W. The minimum lift-off area (MLA) was determined by the

tangent line of the liquid-expanded area linear extrapolation to 0 mN $\cdot$ m $^{-1}$ . The LB film was prepared by a vertical deposition. A hydrophilic substrate was dipped into the subphase before spreading the protein solution. The protein monolayer was deposited in an upstroke at a desired surface pressure at a rate of 4.5 mm $\cdot$ min $^{-1}$ . Experiments were carried out at a temperature of  $25 \pm 0.5$  °C.

**Characterizations.** For characterizations such as CD, FTIR, and AFM, the film samples are to be prepared. As mentioned in the previous paragraph, the LB films of proteins can be deposited on a substrate (ZnSe crystal, quartz slide, glass slide) at a particular surface pressure if the protein molecules can form a Langmuir monolayer. Films were prepared by immersing the substrate in a protein solution for a period of time if the protein cannot form into a Langmuir layer due to the low concentration. The measurement was conducted after drying in a blow of  $\text{N}_2$ . The morphology of protein films was observed under an atomic force microscope, Nanoscope IIIa (Digital Instruments). The tapping mode was applied. ATR-FTIR spectra were collected on a Bruker IFS 66 v/s Spectrometer. The FTIR spectra were registered between 4000 and 400 cm $^{-1}$ , with 128 scans per spectrum at an established standard resolution of 4 cm $^{-1}$ . CD measurements were performed on an applied photophysics spectro-polarimeter equipped with a temperature controller (JASCO-715). All of the CD measurements were conducted at  $\sim 25$  °C with an accuracy of  $\pm 0.5$  °C. The instrument was calibrated with MQ water using a quartz cuvette with a path length of 10 mm or a blank quartz slide. Spectra were collected with a scan speed of 50 nm $\cdot$ min $^{-1}$  with a spectral bandwidth of 10 nm. Each spectrum was the average of four scans. The result was expressed as a mean residue ellipticity in deg $\cdot$ cm $^2$  $\cdot$ mol $^{-1}$ , which is defined as  $\alpha$ -helical,  $\beta$ -sheet,  $\beta$ -turn, and random coil. The percentage of each component was determined by using the curve-fitting method of the far UV CD spectrum linked with the JASCO secondary structure manager.<sup>30</sup>

**Fabrication of the Working Electrode.** The working electrode (WE) was a homemade silver solid amalgam electrode (sSAE) which has a geometric area of 0.50 mm $^2$ . The silver solid amalgam paste was made by mixing silver powder with mercury (1:3, w/w), and the paste was loaded in a cavity (10 mm in depth) of a hollow tube of polystyrene. The sSAE was tightly impacted after the silver amalgam grows into a solid state, and the sSAE was connected with a copper wire at one end. The electrode was cleaned by polishing on an emery paper of 1000 grit followed by ultrasonic treatment and copious DI water rinsing. Prior to use, the electrode was further polished with nanosized KCl powders to clean up the possible oxide layer. Finally, the electrode was subjected to repetitive potential cycling between  $-2.0$  and  $-1.6$  at 0.1 V $\cdot$ s $^{-1}$  in PBS until a zero background current was obtained.

**Electrochemical Measurements.** Electrochemical measurements were performed on an AUTOLAB 302N potentiostat (EcoChemie, The Netherlands) in connection with a three-electrode system. A Ag/AgCl (3.0 M KCl) electrode as the reference electrode and a platinum wire as the auxiliary electrode were utilized. All experiments were carried out with absence of oxygen. The temperature for these experiments is  $25.0 \pm 0.5$  °C. The analyte BSA was adsorbed on the surface of the WE by immersing the sSAE in the BSA solutions for 1.0 min. The BSA-modified electrode was immediately transferred to the PBS electrolyte in a thermostated electrolytic cell, followed by recording of chronopotentiograms or voltammo-

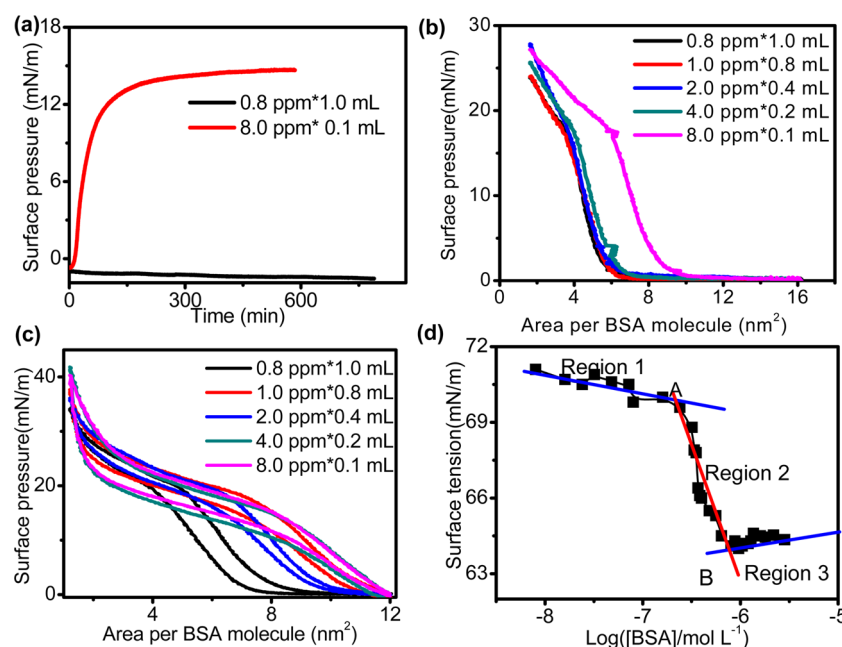


**Figure 1.** (a) Surface pressure vs time ( $\pi$ - $t$ ) kinetics after spreading BSA aqueous solutions of different concentrations but with the same amount ( $8.0 \times 10^{-4}$  mg) over the water subphase (190.0 mL). (b)  $\pi$ - $A$  isotherms for monolayers of BSA obtained after equilibrium time (6 h). (c) Cycles of compression/decompression isotherms of the BSA Langmuir layer by spreading BSA aqueous solutions on the MQ water subphase. (d) Dependence of the surface tension,  $\gamma$ , on  $\log[\text{BSA}]$  in the MQ water subphase (pH 6.8–7.2) with different protein concentrations ( $[\text{BSA}]$ ) at a temperature of  $25 \pm 0.5$  °C.

grams. When the CPS was recorded, a constant stripping current ( $I_{\text{str}} = 10$   $\mu\text{A}$ ) was applied, and the recorded  $E$ - $t$  dependence was automatically converted to a  $(dE/dt)^{-1}$  vs  $E$  curve. The scanning rate was  $0.05$   $\text{V}\cdot\text{s}^{-1}$ . Prior to the scan, a blank experiment was performed by scanning the sSAE in PBS solution ( $0.02$  M, pH 7.0) to make sure all the surfaces of sSAE were cleaned.

## RESULTS AND DISCUSSION

Herein, we fixed the protein amount in the spreading solutions but diluted the BSA into different concentrations. For example, two typical aqueous solutions with concentrations of  $8.0$  ppm ( $0.1$  mL) and  $0.8$  ppm ( $1.0$  mL), sharing the same amount  $8.0 \times 10^{-4}$  mg ( $1.2 \times 10^{-11}$  mol), were spread on a volume of  $190$  mL of MQ water subphase, respectively. The surface pressure was surveyed as a function of time ( $\pi$ - $t$ ) after spreading. We found totally different behaviors of  $\pi$ - $t$  kinetics curves (Figure 1a). The surface pressure of the interface constructed with the  $8.0$  ppm spreading solution experiences a short disturbance at the initial period of  $\sim 5.0$  min. Subsequently, the surface pressure rises along an exponential functional profile (red curve), and finally stabilizes at  $\sim 15.0$  mN/m for a long duration ( $>6.0$  h). However, the lower concentrated ( $0.8$  ppm) protein solution does not show any surface activity; i.e., the surface pressure exhibits a steady decreasing trend during the same period of the elapsing time (Figure 1a, black curve). It is usually believed that the final two solutions after equilibrium should be the same with respect to the concentration of protein ( $\sim 6.3 \times 10^{-11}$  M) in the subphase; however, the reproducibility of our findings, this abnormal phenomenon, is a sign that these two spreading solutions could have different conformations in the protein molecule. The increase of  $\pi$  suggests the formation of a protein Langmuir monolayer at the A/W interface. However, the construction of the Langmuir layer depends on the starting concentration of the spreading protein solution even if the total

amount of protein added is the same. We thus performed detailed experiments by diluting the concentration between  $8.0$  and  $0.8$  ppm while increasing the volume of the spreading solutions (Figure S1a, Supporting Information). For example, the solutions,  $4.0$  ppm  $\times 0.2$  mL,  $2.0$  ppm  $\times 0.4$  mL, and  $1.0$  ppm  $\times 0.8$  mL, were spread over the same volume of subphase ( $190$  mL of water). The  $\pi$ - $t$  curves recorded are displayed in Figure S1a in the Supporting Information. At a concentration of  $1.0$  ppm, the  $\pi$ - $t$  remains as a horizontal curve at a pressure of  $0$  mN/m. This suggests that BSA molecules of this concentration tend to be strongly solubilized in the subphase. We therefore indicate a critical concentration of ca.  $1.0$  ppm that is ascribed to the structural conformational transition or the construction of the BSA Langmuir monolayer. Below this critical concentration, BSA molecules are almost solubilized in the subphase and no excess BSA molecules remain at the A/W interface to arrange into a monolayer. Above this critical concentration, we have studied the thermodynamics and kinetics of the protein adsorption at the A/W interface. By fitting the  $\pi$ - $t$  kinetics curves, we have derived parameters of the rate constant ( $k$ ), decay lifetime ( $\tau_{1/e}$ ), partition coefficient ( $K_d$ ), i.e., the proportion of superficial protein molecules to those solubilized in the subphase, and molar Gibbs free energy change ( $\Delta G$ ). The fitting method was reported elsewhere.<sup>27</sup> Examples of calculations (termed as method I) are detailed in the Supporting Information (section 1.1), and results are also summarized in the Supporting Information (Table S1). As can be found, the values  $-\Delta G$  for the protein adsorption by Langmuir layers are always lower than  $10$   $\text{kJ}\cdot\text{mol}^{-1}$ . This suggests the weak bonding forms in the adsorption process which might include hydrogen bonding, electrostatic, hydrophobic, and/or van der Waals forces.<sup>31</sup> Figure 1b shows the surface pressure vs area ( $\pi$ - $A$ ) isotherms by compressing the BSA monolayers after equilibrium. All of the isotherms have a similar shape, in which two phase transitions (gas to liquid-



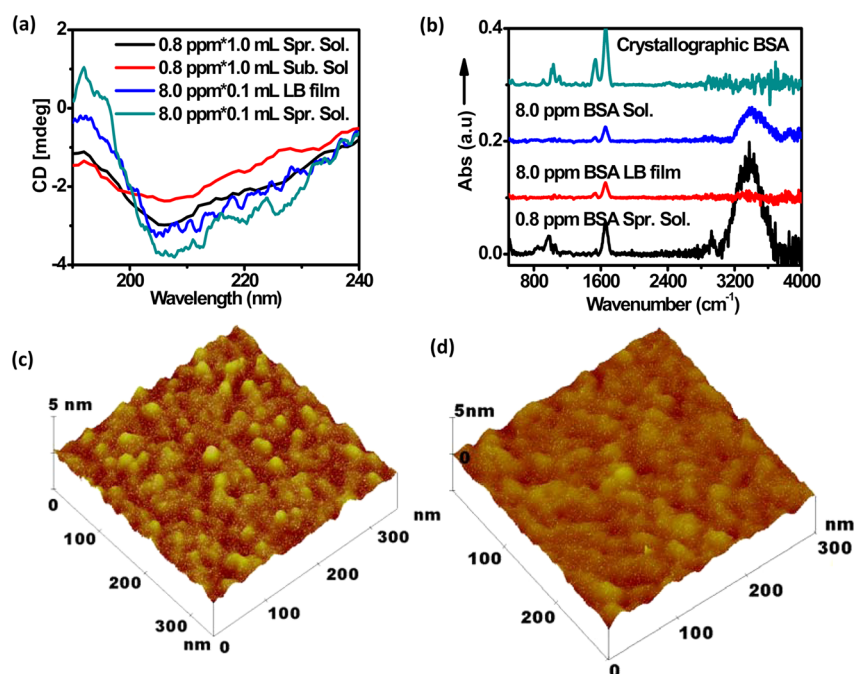


**Figure 2.** (a) CD and (b) ATR-FTIR spectra of BSA spreading solutions (Spr. Sol.) with concentrations of 0.8 and 8.0 ppm, or their corresponding LB (adsorbed) films. The FTIR measurement of BSA adsorbed film (0.8 ppm) is performed by immersing an internal reflection element (ZnSe crystal) in the 0.8 ppm BSA solution for 10 min. The sample was prepared by N<sub>2</sub> blowing. (c) AFM image of BSA LB film prepared by spreading BSA aqueous solution (8.0 ppm × 0.1 mL) over a 190 mL water subphase. The deposition surface pressure is 2.0 mN/m. (d) AFM image of the adsorbed BSA prepared in a subphase (190 mL of water) with addition of BSA solution (0.8 ppm × 1.0 mL).

expanded [LE]; LE to liquid-condensed [LC]) pressure can be found at about 0.0 and 14.6 mN/m, respectively. The minimum lift-off areas (MLA) which were defined by the tangent line of the LE area are found to vary within 5.4–11.0 nm<sup>2</sup> per molecule. A higher concentration (8.0 ppm) exhibits a larger MLA (9.0–11.0 nm<sup>2</sup>), while lower concentrated BSA spreading solution (2.0 ppm) gives a smaller MLA at 5.4–6.2 nm<sup>2</sup>. The MLA was calculated on the basis that all proteins added remain at the interfacial layer. Therefore, the MLA value does not represent the truth of the cross-sectional area for a protein molecule at the A/W interface.<sup>23</sup> The reason lies in the fact that only a portion of the BSA molecules are stabilized at the A/W interface while the remaining protein molecules are solubilized in the subphase. According to  $K_d$ , we might calculate the amount of protein molecules ( $n_{\text{surf}}$  unit: mol) that stay at the A/W interface and those being solubilized in the subphase. We thus obtained the cross-sectional area per BSA molecule ( $A_{\text{sec}}$ ) based on the following equation:  $A_{\text{sec}} = 1.46 \times 10^{16} / (n_{\text{surf}} \times N_A)$ , where  $1.46 \times 10^{16}$  (unit: nm<sup>2</sup>) is the area of the A/W interface (Langmuir trough) and  $N_A$  is the Avogadro constant. We obtained a growing trend of  $A_{\text{sec}}$  when the protein solution becomes diluted (Table S1, Supporting Information). Similar results of MLA were also found by Moyá et al., in which the authors studied the packing state of BSA mixed with external surfactants.<sup>32</sup> The hysteresis under successive compression/decompression cycles was reproducible for all concentrations higher than 1.0 ppm (Figure 1c), and this reflects the elastic characteristics of protein layers. The nonrigid Langmuir monolayer might originate from the softness of macromolecules which are produced in a process of protein folding upon dilution.<sup>33</sup> As is known, the addition of inorganic salts strongly accelerates the protein adsorption at the expense of shielding electrostatic repulsions.<sup>25</sup> To confirm interactions due to the electrostatic forces, we constructed Langmuir layers over

PBS ( $I = 0.02$  M), in which the pH value was set at 4.0 and 7.2, respectively. Figures S2 and S3 of the Supporting Information display the  $\pi$ - $t$  kinetics curves and  $\pi$ - $A$  isotherms over the buffer solutions. A critical concentration was found at 0.1–0.2 ppm irrespective of the pH values in the PBS subphase. This lower critical concentration is indicative of less solubilization of BSA in the buffer subphases. The assembly of BSA molecules is not influenced by the electrostatic forces imposed by the charged BSA molecules. As is known, the isoelectric points of BSA lie between pH 4.7 and 5.6; therefore, the BSA molecules show different charges in the two subphases at pH 4.2 and 7.2.<sup>34</sup> The electrostatic forces were thus ruled out to be responsible for the protein unfolding in such cases. It has been reported that the addition of surfactants would aid the formation of the critical micellar concentration (cmc) of BSA in aqueous solutions.<sup>35</sup> Herein, we found that the cmc of BSA can be obtained in the aqueous subphases even without the assistance of surfactants. We performed surface tension ( $\gamma$ ) measurements by varying the protein concentrations as well as the amounts (see Figure 1d in the main manuscript and Figure S4 in the Supporting Information). Figure 1d shows the dependence of  $\gamma$  on  $\log[\text{BSA}]$  for the aqueous solutions, where the [BSA] is the concentration of protein in the subphase.<sup>35</sup> The slope of the linear (region 2, red line) is a measure of the interfacial adsorption efficiency of BSA molecules, which can be quantified by the surface excess concentration ( $\Gamma_{\text{max}}^{\text{cmc}}$ ). Details of calculations (termed as method II) are presented in the Supporting Information (section 4). The partition coefficient was evaluated to be 0.318 ( $-\Delta G = 2.84$  kJ·mol<sup>-1</sup>, Table S1, Supporting Information), which is in agreement with what has been determined from the analysis (0.32) of  $\pi$ - $t$  kinetic curves, as stated in method I. These results demonstrate there are phase transitions in the Langmuir monolayers before the

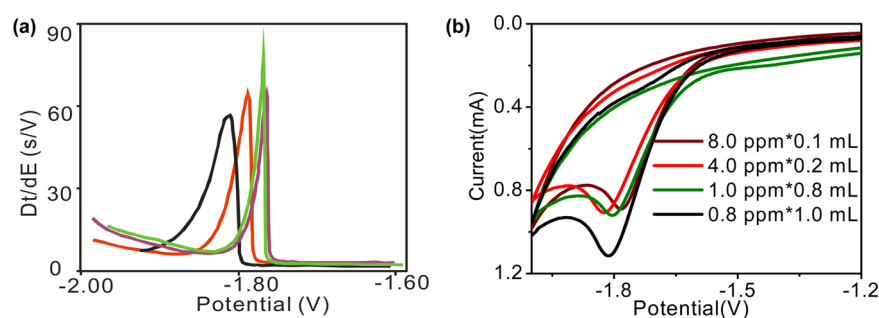


**Figure 3.** (a) CPS peak H and (b) CV profiles with peaks close to  $-1.8$  V of the BSA aqueous solutions which was prepared by spreading different concentrations of BSA stock solutions. Chronopotentiograms were recorded in the PBS electrolyte ( $I = 0.02$  M) at pH  $\sim 7.0$ . The concentrations including 0.8, 1.0, 4.0, and 8.0 ppm were spread at a temperature of  $25 \pm 0.5$  °C.

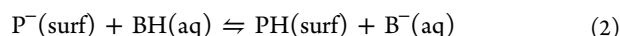
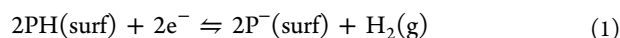
formation of cmc, and the concentration is lower than the cmc as indicated by point A (Figure 1d).

To probe the structural changes of BSA molecules induced by concentrations, the CD spectra were examined to ascertain the protein secondary structure of the two typical solutions. Figure 2a shows the CD spectra (190–240 nm) of BSA LB films and spreading solutions. The weights of the secondary structure ( $\alpha$ -helix,  $\beta$ -sheet,  $\beta$ -turn, and random coil) of BSA are listed in Table S2 (see the Supporting Information). For a concentration of 8.0 ppm, either the spreading solutions or its LB film, the CD spectrum contains two negative minima of 208 and 221 nm, and a positive peak at 193 nm which are characteristics of a high content of  $\alpha$ -helix. The content of  $\alpha$ -helix in 8.0 ppm solution or its LB film was evaluated to be 31–36%, which is much higher than that of solutions with 0.8 ppm concentration (9–14%). Although the percentage of  $\alpha$ -helix in the 8.0 ppm solutions is less than the reported percentage in the crystallographic structure of BSA (67%  $\alpha$ -helix),<sup>36</sup> it can still indicate a certain native structure remains at this concentration. We did not find the peak of 193 nm in 0.8 ppm BSA solutions, and this suggests that BSA essentially assumes a disordered structure or a lesser content of  $\alpha$ -helix at this concentration.<sup>37</sup> It was believed that a red shift in the CD band (208 nm) denotes the presence of hydrogen-bonding interactions, e.g., bonds between the deprotonated carboxylic acid and head-group surfactants.<sup>38</sup> Herein, we also observed this type of shift which further illustrates that the intramolecular bonds are disrupted, and residual groups of protein would combine with water molecules. This kind of bonding follows a similar way between surfactants and proteins as reported by the literature.<sup>38</sup> The new bonds could produce an extended disordered structure in the protein molecule. We also utilized ATR-FTIR spectroscopy to characterize films formed at the A/W interface. As can be seen in Figure 2b, both amide I ( $-\text{C}=\text{O}$ ) and II ( $-\text{C}=\text{N}$  coupled with  $\text{N}-\text{H}$ ) peaks were found at 1658 and 1550  $\text{cm}^{-1}$ , respectively, in samples of crystallographic BSA (lyophilized powders buried in KBr), 8.0 ppm concentrated spreading solution, and its LB films. However, the band of amide II in the sample of 0.8 ppm was very weak, or the relative intensity with respect to amide I was almost invisible in this sample. This suggests a structural difference of BSA molecules occurs in the sample of 0.8 ppm.<sup>39</sup> Compared to the 8.0 ppm solution, the 0.8 ppm BSA shows a broader amide I band and a red-shift from 1658 to 1651  $\text{cm}^{-1}$ . A prominent hydration effect can be deduced from the greater weight of  $\text{H}-\text{O}-\text{H}$  bending vibration located at 1640  $\text{cm}^{-1}$  in the sample of 0.8 ppm. In order to clarify the content of protein secondary structure, the analysis by curve fitting has been performed in a wavelength of

1485–1730  $\text{cm}^{-1}$  (Figure S5 and Table S3 in the Supporting Information). Peaks at 1650–1655  $\text{cm}^{-1}$  ( $\alpha$ -helices), 1663–1685  $\text{cm}^{-1}$  ( $\beta$ -sheet or  $\beta$ -turn), 1644–1648  $\text{cm}^{-1}$  (random chains), and 1621–1639  $\text{cm}^{-1}$  (extended chains plus  $\beta$ -sheet and side chain moieties) have been assigned.<sup>39</sup> Obviously the percentages of  $\beta$ -sheet and random chains in the 0.8 ppm BSA were higher than those in 8.0 ppm protein solution or its LB film. This indicates an unfolding of BSA molecules was obtained due to the effect of hydration. The more prominent stretching at 3400  $\text{cm}^{-1}$  found in 0.8 ppm BSA also refers to the presence of the  $-\text{OH}$  attached to  $=\text{N}-\text{H}$  groups.<sup>40</sup> Figure 2c displays the AFM image of a LB film prepared by spreading 8.0 ppm BSA solutions over MQ water. Figure 2d shows the AFM image of the sample that was obtained by immersing the substrate in the subphase added by 0.8 ppm protein solution. We found that the LB film was densely composed of numerous small bean-shaped granules. The diameter of the granules is around 25 nm, and the peak–valley height lies within 2.77 nm. This is indicative for self-assembly of BSA aggregations in the LB film.<sup>25</sup> In contrast, the surface of the film prepared from lower concentration gives a much flatter morphology, and the peak–valley height is only 1.98 nm. The roughness of the surface can be summarized by the root-mean-square roughness ( $R_{\text{ms}}$ ), in which we found that the  $R_{\text{ms}}$  of Figure 2c is 0.316 nm and the  $R_{\text{ms}}$  of Figure 2d is 0.252 nm, which clearly demonstrates a rougher surface of the LB film. Figure S6 in the Supporting Information displays the topographical image and phase diagram of the two BSA films, and these further confirm the presence of a heterogeneous morphology at a higher concentration. Although the BSA molecules are suspected to undergo an additional conformational change when we transferred the Langmuir monolayer from the A/W interphase or solubilized BSA molecules to a solid substrate for AFM characterization, these obvious differences in morphologies (Figure 2c and d) give a reflection of structural difference over the two concentrations.

To confirm our indication on the conformation transitions of BSA molecules induced by concentration, we utilized the catalytic hydrogen evolution reaction (HER), which is the most sensitive electrochemical reaction for the protein analysis (Figure 3).<sup>41</sup> The investigation was performed by varying the BSA concentration that was approached by the surface of the WE. For each concentration used in this study (0.8, 1.0, 4.0, or 8.0 ppm), different CPS responses were explained by the accessibility of catalytically active groups and the organization of protein molecules at the WE.<sup>14</sup> Structural differences caused by the concentration would affect the motion of the active groups for the electrochemical process. Although the catalytic

mechanism is not yet unequivocally established, the HER can be satisfactorily described by the following set of reactions:



where PH and  $\text{P}^-$  represent protonated and unprotonated amino acid residues in BSA, respectively; BH is the acid component of the electrolyte, and  $\text{B}^-$  is its conjugate base. The symbols in parentheses represent the state of the molecule ("g" stands for gaseous, "aq" for aqueous, and "surf" for surface confined). Figure 3a shows CPS profiles measured at  $\sim 25.0^\circ\text{C}$ , in which all of the adsorbed BSA yields a well-developed peak HER at around  $-1.90\text{ V}$  vs Ag/AgCl (3.0 M, KCl). The lower concentrated BSA was found to have a more negative peak position compared to that of higher concentration. The negative shift (shown also by the cyclic voltammetry (CV) profile in Figure 3b) implies less accessibility of active groups of the protein.<sup>41</sup> As is known, two requirements must be fulfilled to obtain a catalytic HER peak: the involved peptides which contain amino acid residues with labile protons (e.g.,  $-\text{SH}$  or  $-\text{NH}_3^+$ ) and the capability of being adsorbed on the electrode surface.<sup>42</sup> It has been shown that arginine (Arg), lysine (Lys), and cysteine (Cys) are catalytically active residues that mainly account for the HER at neutral pH.<sup>42,43</sup> Herein, on the basis of the analysis of surface chemistry, the concentration of BSA below 1.0 ppm undergoes an unfolded/denatured transition, and this would make amino acid residues more accessible to the solvents.<sup>44,45</sup> It can be expected that denatured BSA would bind with water molecules as compared to native BSA because of the larger number of binding sites in the unfolded protein. The presence of intramolecular hydrogen bonding would block the N-terminus in the unfolded BSA and perhaps change their orientation at the electrode surface.<sup>46</sup> As a result, less activity of amino acid residues is available for the electrocatalytic process in the case of the expanded structure (0.8 ppm BSA). We suggest that to reserve a better catalytic activity of BSA a concentration higher than 1.0 ppm should be necessarily prepared in an aqueous solution.

It has been reported that part of the amino acids in the primary structure of proteins tend to hydrolyze in the presence of water molecules.<sup>47</sup> In native protein molecules, the hydrophobicity and hydrogen bonds (HBs) are believed to be the main forces to stabilize the globular protein and to hold the folded peptide strands.<sup>3,5,6,47,48</sup> Herein, the intramolecular bonds in the native protein molecules could probably be disrupted due to the presence of the water molecules in such diluted solutions.<sup>49,50</sup> The electronegative atoms (O and N) which used to be buried inside the  $\alpha$ -helixes would be torn apart, and are to be exposed to water molecules to form extra-molecular HBs. We assume that the new-formed extra-molecular HBs account for the unfolding of the BSA molecules, which leads to a high percentage of the random coil in a disordered state of peptides. The BSA molecules become unfolded and expanded, as confirmed by the molecular cross-sectional area and the spectroscopy. In a view of energy ( $-\Delta G$ ), Hammen et al. have drawn that the three HBs lost in a Ser-Ala mutant protein would contribute a Gibbs free energy of  $4.5\text{ kJ}\cdot\text{mol}^{-1}$ .<sup>51</sup> Our results, as obtained from both methods I and II ( $1.0$ – $4.7\text{ kJ}\cdot\text{mol}^{-1}$ ), are in good agreement with those reported data. However, one may attribute the change of the cross-sectional area ( $A_{\text{sec}}$ ) of BSA molecules to a different orientation (e.g., the end-on or side-on adsorption). Herein, we

can ignore this effect because the concentration ( $6.3 \times 10^{-11}\text{ M}$ ) of BSA studied in this research is much lower than those in the previous reports.<sup>52,53</sup> BSA molecules are considered as a type of "soft" proteins which tend to be deformed from its original heart shape when it was adsorbed on a surface or was dissolved in a solution.<sup>54</sup> Under such low concentration, the deformation of BSA molecules could happen before they were immobilized on the substrates (ZnSe crystal, quartz slide, glass slide). As pointed out by Rezwan et al.,<sup>21</sup> the relaxation of the BSA molecules was mainly attributed to the combined effects of stacking faults and changes of molecular structures. The stacking fault or the orientation is more prominent in determining  $A_{\text{sec}}$  when the BSA was adsorbed from a higher concentration solution ( $>0.1\text{ g}\cdot\text{L}^{-1}$ ). In low concentration, the relaxation could result in an increase of  $A_{\text{sec}}$  which was mainly ascribed to the structural variations of the protein molecules. Furthermore, in the literature of Satoshi Fukuzaki's,<sup>53</sup> the  $A_{\text{sec}}$  of BSA molecules could be quite different if the protein molecules were adsorbed as a flat configuration and a close packed configuration. However, we got similar values of  $A_{\text{sec}}$  of BSA at different concentrations (Table S1, Supporting Information). Therefore, the effect of orientations for BSA molecules can be ignored in such diluted solutions. To further confirm our hypothesis, an experiment of  $\pi$ - $t$  kinetics was recorded during which the urea in the form of solutions was added. As is known, urea would compete with water to form a stronger hydrogen-bonding network with BSA, thereby triggering a disturbance in the surface pressure of the Langmuir layer.<sup>55</sup> The  $\pi$ - $t$  curve is presented in Figure S7 (see the Supporting Information). As can be seen, the surface pressure decreases due to the addition of urea, which reflects the denaturation of BSA induced by urea. This behavior is similar to the trend of  $\pi$  over the low concentrated subphase induced by water, although the rate of  $\pi$  change is much faster, and this suggests that stronger HBs are formed between BSA and urea molecules than those between BSA and water. The experiment reveals that water molecules can have a similar role as urea in denaturing BSA molecules.

## CONCLUSIONS

In conclusion, the unfolding of BSA molecule in aqueous solution at neutral pH which is solely induced by the concentration was disclosed by surface chemical, spectroscopy, and electrochemical characterizations. Two critical concentrations have been determined at about 1.0 and 0.2 ppm when the BSA molecules are dissolved in water and PBS ( $I = 0.02\text{ M}$ ) solutions. The conformational change is mainly due to the extra-molecular hydrogen bonds formed between polar groups of unfolded BSA and water molecules. Parameters of kinetics including time constant ( $\tau_{1/e}$ ) and rate constant ( $k$ ) as well as those of thermodynamics including partition coefficient ( $K_d$ ) and molar Gibbs free energy change ( $\Delta G$ ) have been determined in the formation of the BSA Langmuir monolayer. The structure of the protein molecule in solutions of concentration across the critical point has been analyzed by CD, ATR-FTIR, AFM, and electrochemical means. This discovery fills in the gaps of Foster's N-F model, in which the conformational change of BSA molecules was influenced by the solvent effects at neutral pH. This research has significance in determining the concentration for a protein solution if one aims to retain the biocatalytic activity.



## ■ ASSOCIATED CONTENT

## ■ Supporting Information

Experimental procedures, sample characterizations, and examples of calculations. This material is available free of charge via the Internet at <http://pubs.acs.org>.

## ■ AUTHOR INFORMATION

## Corresponding Author

\*E-mail: miaosd@iccas.ac.cn. Phone: 86-551-62901560.

## Notes

The authors declare no competing financial interest.

## ■ ACKNOWLEDGMENTS

The authors are grateful to Prof. Robert A. Schoonheydt for useful discussions when the behavior of interfacial BSA molecules was first discovered in his lab (Center for Surface Chemistry and Catalysis, K.U. Leuven, Belgium). This research was financially supported by the National Natural Science Foundation of China (21103039), Research Fund for the Doctoral Program of Higher Education of China (20110111120008), Anhui Provincial Natural Science Foundation for Distinguished Young Scholars (1408085J06), and the Beijing National Laboratory for Molecular Sciences (J2014KJZS0202).

## ■ REFERENCES

- (1) Bhattacharya, M.; Jain, N.; Bhasne, K.; Kumari, V.; Mukhopadhyay, S. pH-Induced Conformational Isomerization of Bovine Serum Albumin Studied by Extrinsic and Intrinsic Protein Fluorescence. *J. Fluoresc.* **2011**, *21*, 1083–1090.
- (2) Fersht, A. R.; Daggett, V. Protein Folding and Unfolding at Atomic Resolution. *Cell* **2002**, *108*, 573–582.
- (3) Pereira, L. G. C.; Theodoly, O.; Blanch, H. W.; Radke, C. J. Dilational Rheology of BSA Conformers at the Air/Water Interface. *Langmuir* **2003**, *19*, 2349–2356.
- (4) Foster, J. F.; Samsa, E. G. Streaming Orientation Studies on Denatured Proteins. I. Heat Denaturation of Ovalbumin in Acid Media. *J. Am. Chem. Soc.* **1951**, *73*, 3187–3190.
- (5) Foster, J. F.; Samsa, E. G. Streaming Orientation Studies on Denatured Proteins. III. Denaturation of Ovalbumin in the Presence of Urea. *J. Am. Chem. Soc.* **1951**, *73*, 5388–5391.
- (6) Khan, M. Y. Direct Evidence for the Involvement of Domain III in the N-F Transition of Bovine Serum Albumin. *Biochem. J.* **1986**, *236*, 307–310.
- (7) Barbosa, L. R. S.; Ortore, M. G.; Spinozzi, F.; Mariani, P.; Bernstorff, S.; Itri, R. The Importance of Protein-Protein Interactions on the pH-Induced Conformational Changes of Bovine Serum Albumin: A Small-Angle X-Ray Scattering Study. *Biophys. J.* **2010**, *98*, 147–157.
- (8) Ahmad, B.; Kamal, M. Z.; Khan, R. H. Alkali-Induced Conformational Transition in Different Domains of Bovine Serum Albumin. *Protein Pept. Lett.* **2004**, *11*, 307–315.
- (9) Bramanti, E.; Ferrari, C.; Angeli, V.; Onor, M.; Synovec, R. E. Characterization of BSA Unfolding and Aggregation Using a Single-Capillary Viscometer and Dynamic Surface Tension Detector. *Talanta* **2011**, *85*, 2553–2561.
- (10) Li, Y.; Mattison, K. W.; Dubin, P. L.; Havel, H. A.; Edwards, S. L. Light Scattering Studies of the Binding of Bovine Serum Albumin to a Cationic Polyelectrolyte. *Biopolymers* **1996**, *38*, 527–533.
- (11) Messina, P.; Prieto, G.; Dodero, V.; Cabrerizo-Vilchez, M. A.; Maldonado-Valderrama, J.; Ruso, J. M.; Sarmiento, F. Surface Characterization of Human Serum Albumin and Sodium Perfluorooctanoate Mixed Solutions by Pendant Drop Tensiometry and Circular Dichroism. *Biopolymers* **2006**, *82*, 261–271.
- (12) Feng, L.; Hu, C. Z.; Andrade, J. D. Scanning Tunneling Microscopic Images of Adsorbed Serum Albumin on Highly Oriented Pyrolytic Graphite. *J. Colloid Interface Sci.* **1988**, *126*, 650–653.
- (13) Wu, H.; Lin, L.; Wang, P.; Jiang, S.; Dai, Z.; Zou, X. Solubilization of Pristine Fullerene by the Unfolding Mechanism of Bovine Serum Albumin for Cytotoxic Application. *Chem. Commun.* **2011**, *47*, 10659–10661.
- (14) Ostatna, V.; Cernocka, H.; Palecek, E. Protein Structure-Sensitive Electrocatalysis at Dithiothreitol-Modified Electrodes. *J. Am. Chem. Soc.* **2010**, *132*, 9408–9413.
- (15) El Kadi, N.; Taulier, N.; Le Huerou, J. Y.; Gindre, M.; Urbach, W.; Nwigwe, I.; Kahn, P. C.; Waks, M. Unfolding and Refolding of Bovine Serum Albumin at Acid pH: Ultrasound and Structural Studies. *Biophys. J.* **2006**, *91*, 3397–3404.
- (16) Santos, S. F.; Zanette, D.; Fischer, H.; Itri, R. A Systematic Study of Bovine Serum Albumin (BSA) and Sodium Dodecyl Sulfate (SDS) Interactions by Surface Tension and Small Angle X-Ray Scattering. *J. Colloid Interface Sci.* **2003**, *262*, 400–408.
- (17) Shen, Y. R.; Ostroverkhov, V. Sum-Frequency Vibrational Spectroscopy on Water Interfaces: Polar Orientation of Water Molecules at Interfaces. *Chem. Rev.* **2006**, *106*, 1140–1154.
- (18) Lajtha, A.; Banik, N.; Szilagyi, A.; Kardos, J.; Osvath, S.; Barna, L.; Zavodszky, P. Protein Folding. In *Handbook of Neurochemistry and Molecular Neurobiology*; Springer: 2007; pp 303–343.
- (19) Richmond, G. L. Molecular Bonding and Interactions at Aqueous Surfaces as Probed by Vibrational Sum Frequency Spectroscopy. *Chem. Rev.* **2002**, *102*, 2693–2724.
- (20) Noskov, B. A.; Mikhailovskaya, A. A.; Lin, S. Y.; Loglio, G.; Miller, R. Bovine Serum Albumin Unfolding at the Air/Water Interface as Studied by Dilational Surface Rheology. *Langmuir* **2010**, *26*, 17225–17231.
- (21) Rezwani, K.; Meier, L. P.; Rezwani, M.; Voros, J.; Textor, M.; Gauckler, L. J. Bovine Serum Albumin Adsorption onto Colloidal Al<sub>2</sub>O<sub>3</sub> Particles: A New Model Based on Zeta Potential and UV-Vis Measurements. *Langmuir* **2004**, *20*, 10055–10061.
- (22) Wang, J.; Buck, S. M.; Chen, Z. The Effect of Surface Coverage on Conformation Changes of Bovine Serum Albumin Molecules at the Air-Solution Interface Detected by Sum Frequency Generation Vibrational Spectroscopy. *Analyst* **2003**, *128*, 773–778.
- (23) Lu, J. R.; Su, T. J.; Thomas, R. K. Structural Conformation of Bovine Serum Albumin Layers at the Air–Water Interface Studied by Neutron Reflection. *J. Colloid Interface Sci.* **1999**, *213*, 426–437.
- (24) McClellan, S. J.; Franses, E. I. Effect of Concentration and Denaturation on Adsorption and Surface Tension of Bovine Serum Albumin. *Colloids Surf., B* **2003**, *28*, 63–75.
- (25) Miao, S.; Leeman, H.; De Feyter, S.; Schoonheydt, R. A. Facile Preparation of Langmuir-Blodgett Films of Water-Soluble Proteins and Hybrid Protein-Clay Films. *J. Mater. Chem.* **2010**, *20*, 698–705.
- (26) Tripp, B. C.; Magda, J. J.; Andrade, J. D. Adsorption of Globular Proteins at the Air/Water Interface as Measured via Dynamic Surface Tension: Concentration Dependence, Mass-Transfer Considerations, and Adsorption Kinetics. *J. Colloid Interface Sci.* **1995**, *173*, 16–27.
- (27) Miao, S.; Leeman, H.; De Feyter, S.; Schoonheydt, R. A. Three-Component Langmuir-Blodgett Films Consisting of Surfactant, Clay Mineral, and Lysozyme: Construction and Characterization. *Chem.—Eur. J.* **2010**, *16*, 2461–2469.
- (28) Miao, S. D.; Bergaya, F.; Schoonheydt, R. A. Ultrathin Films of Clay-Protein Composites. *Philos. Mag.* **2010**, *90*, 2529–2541.
- (29) Miao, S. D.; Qiu, Z. G.; Cui, P. Clay-Protein Ultrathin Films: Design and Bio-Catalytic Performance Study. *Sci. China: Chem.* **2012**, *55*, 1842–1855.
- (30) Greenfield, N. J. Using Circular Dichroism Spectra to Estimate Protein Secondary Structure. *Nat. Protoc.* **2006**, *1*, 2876–2890.
- (31) Ye, W.; He, S.; Ding, L.; Yao, Y.; Wan, L.; Miao, S.; Xu, J. Supported Ionic-Liquid “Semi-Heterogeneous Catalyst”: An Interfacial Chemical Study. *J. Phys. Chem. C* **2013**, *117*, 7026–7038.
- (32) Martín, V. I.; Rodríguez, A.; Maestre, A.; Moyá, M. L. Binding of Cationic Single-Chain and Dimeric Surfactants to Bovine Serum Albumin. *Langmuir* **2013**, *29*, 7629–7641.

- (33) Pedraz, P.; Montes, F. J.; Cerro, R. L.; Díaz, M. E. Characterization of Langmuir Biofilms Built by the Biospecific Interaction of Arachidic Acid with Bovine Serum Albumin. *Thin Solid Films* **2012**, *525*, 121–131.
- (34) Engelhardt, K.; Rumpel, A.; Walter, J.; Dombrowski, J.; Kulozik, U.; Braunschweig, B.; Peukert, W. Protein Adsorption at the Electrified Air–Water Interface: Implications on Foam Stability. *Langmuir* **2012**, *28*, 7780–7787.
- (35) Chakraborty, T.; Chakraborty, I.; Moulik, S. P.; Ghosh, S. Physicochemical and Conformational Studies on BSA–Surfactant Interaction in Aqueous Medium. *Langmuir* **2009**, *25*, 3062–3074.
- (36) He, X. M.; Carter, D. C. Atomic Structure and Chemistry of Human Serum Albumin. *Nature* **1992**, *358*, 209–215.
- (37) Clark, A. H.; Saunderson, D. H.; Suggett, A. Infrared and Laser-Raman Spectroscopic Studies of Thermally-Induced Globular Protein Gels. *J. Pept. Protein Res.* **1981**, *17*, 353–364.
- (38) Singh, T.; Bharmoria, P.; Morikawa, M.-a.; Kimizuka, N.; Kumar, A. Ionic Liquids Induced Structural Changes of Bovine Serum Albumin in Aqueous Media: A Detailed Physicochemical and Spectroscopic Study. *J. Phys. Chem. B* **2012**, *116*, 11924–11935.
- (39) Roach, P.; Farrar, D.; Perry, C. C. Interpretation of Protein Adsorption: Surface-Induced Conformational Changes. *J. Am. Chem. Soc.* **2005**, *127*, 8168–8173.
- (40) Lad, M. D.; Birembaut, F.; Frazier, R. A.; Green, R. J. Protein-Lipid Interactions at the Air/Water Interface. *Phys. Chem. Chem. Phys.* **2005**, *7*, 3478–3485.
- (41) Ostatná, V.; Uslu, B.; Dogan, B.; Ozkan, S.; Paleček, E. Native and Denatured Bovine Serum Albumin. D.c. Polarography, Stripping Voltammetry and Constant Current Chronopotentiometry. *J. Electroanal. Chem.* **2006**, *593*, 172–178.
- (42) Doneux, T.; Dorčák, V.; Paleček, E. Influence of the Interfacial Peptide Organization on the Catalysis of Hydrogen Evolution. *Langmuir* **2009**, *26*, 1347–1353.
- (43) Paleček, E.; Ostatná, V. Electroactivity of Nonconjugated Proteins and Peptides. Towards Electroanalysis of All Proteins. *Electroanalysis* **2007**, *19*, 2383–2403.
- (44) Ostatná, V.; Paleček, E. Native, Denatured and Reduced BSA: Enhancement of Chronopotentiometric Peak H by Guanidinium Chloride. *Electrochim. Acta* **2008**, *53*, 4014–4021.
- (45) Ostatná, V.; Kuralay, F.; Trnková, L.; Paleček, E. Constant Current Chronopotentiometry and Voltammetry of Native and Denatured Serum Albumin at Mercury and Carbon Electrodes. *Electroanalysis* **2008**, *20*, 1406–1413.
- (46) Manning, M. C.; Patel, K.; Borchardt, R. T. Stability of Protein Pharmaceuticals. *Pharm. Res.* **1989**, *6*, 903–918.
- (47) Carter, D. C.; Ho, J. X. Structure of Serum Albumin. *Adv. Protein Chem.* **1994**, *45*, 153–203.
- (48) Pace, C. N.; Shirley, B. A.; McNutt, M.; Gajiwala, K. Forces Contributing to the Conformational Stability of Proteins. *FASEB J.* **1996**, *10*, 75–83.
- (49) Rodríguez Niño, M. R.; Rodríguez Patino, J. M. Effect of the Aqueous Phase Composition on the Adsorption of Bovine Serum Albumin to the Air–Water Interface. *Ind. Eng. Chem. Res.* **2002**, *41*, 1489–1495.
- (50) Tang, C.-H.; Shen, L. Role of Conformational Flexibility in the Emulsifying Properties of Bovine Serum Albumin. *J. Agric. Food Chem.* **2013**, *61*, 3097–3110.
- (51) Hammen, P. K.; Scholtz, J. M.; Anderson, J. W.; Waygood, E. B.; Klevit, R. E. Investigation of a Side-Chain-Side-Chain Hydrogen Bond by Mutagenesis, Thermodynamics, and NMR Spectroscopy. *Protein Sci.* **1995**, *4*, 936–944.
- (52) Kondo, A.; Murakami, F.; Higashitani, K. Circular Dichroism Studies on Conformational Changes in Protein Molecules upon Adsorption on Ultrafine Polystyrene Particles. *Biotechnol. Bioeng.* **1992**, *40*, 889–894.
- (53) Urano, H.; Fukuzaki, S. Conformation of Adsorbed Bovine Serum Albumin Governing Its Desorption Behavior at Alumina–Water Interfaces. *J. Biosci. Bioeng.* **2000**, *90*, 105–111.
- (54) Dickinson, E. Adsorbed Protein Layers at Fluid Interfaces: Interactions, Structure and Surface Rheology. *Colloids Surf., B* **1999**, *15*, 161–176.
- (55) Kumaran, R.; Ramamurthy, P. Denaturation Mechanism of BSA by Urea Derivatives: Evidence for Hydrogen-Bonding Mode from Fluorescence Tools. *J. Fluoresc.* **2011**, *21*, 1499–1508.